SCIENCE CHINA
Earth Sciences

•ARTICLE•

March 2025 Vol.68 No.3: 898–908
https://doi.org/10.1007/s11430-024-1506-4

# The global 64-year sea level oscillation and its possible external excitation sources

Mingyu XIAO[1], Taoyong JIN[1,2*], Hao DING[1,2*], Lianjun YANG[1], Xiaolong LI[1] & Jiancheng LI[1,2]

[1] *School of Geodesy and Geomatics, Wuhan University, Wuhan 430079, China*
[2] *MOE Key Laboratory of Geospace Environment and Geodesy, Wuhan University, Wuhan 430079, China*

Received March 12, 2024; revised December 13, 2024; accepted December 30, 2024; published online February 17, 2025

**Abstract** Low-frequency signals play an important role in understanding sea level changes and their acceleration. This paper analyzed multidecadal oscillations on a global scale with tide gauge records. A significant stable oscillation of approximately 64 years was identified at 177 globally distributed tide gauges, with an estimated period of 63±4 yr. The amplitude of this oscillation depends on latitude, whereas the phase depends on longitude. The regions most affected (up to ~20 mm) by the 64-yr oscillation include Europe, North America, South Australia, and East Asia. Our results are consistent with the spherical harmonic model, indicating that the 64-yr oscillation is not a random or irregular signal but rather a global signal likely excited by a specific source. To explore the possible excitation sources, we analyzed several external factors closely related to sea level change (where "external" refers to factors relative to the Earth's interior), including thermosteric sea level, ocean mass change, precipitation, sea level pressure, surface temperature, sunspot numbers, solar flux, and the total solar irradiance index. Our results show that there are significant differences in the periods, amplitudes and phases of the multidecadal characteristics of these datasets from those of the 64-yr oscillation; thus the existence of the 64-yr oscillation was denied in these datasets. Therefore, we firstly confirm that climate change and solar activity cannot explain the 64-yr sea level oscillation.

**Keywords** Sea level change, 64-year oscillation, Tide gauge records, Solar activity, Climate change

**Citation:** Xiao M, Jin T, Ding H, Yang L, Li X, Li J. 2025. The global 64-year sea level oscillation and its possible external excitation sources. Science China Earth Sciences, 68(3): 898–908, https://doi.org/10.1007/s11430-024-1506-4

## 1. Introduction

Sea level change is essential to human economic life in low-elevation coastal areas. While numerous studies have focused on relatively high-frequency signals shorter than 10 years such as seasonal, annual, and interannual sea level changes, research on relatively low-frequency signals longer than 10 years remains insufficient. As a critical component of sea level change, low-frequency signals cannot be ignored when estimating sea level rise and its acceleration. For example, interdecadal changes significantly affect the estimation of acceleration when the sea level record is shorter than 50 years (Douglas, 1992); more than 60/100 years of records are needed to compute a reliable sea level rise rate/acceleration (Boretti, 2020). Low-frequency signals are also the key to explaining the differences in the estimated parameters of sea level change. For example, the global mean sea level (GMSL) rise rate obtained from satellite altimetry data over the past 30 years is larger than that since the 1960s and is nearly twice that from tide gauge data since 1900 (Cazenave and Moreira, 2022). This acceleration is suspected to be at least partially caused by multidecadal changes (Iz et al., 2018), but an accurate quantitative explanation needs to be verified. However, the acknowledged low-frequency signals

* Corresponding authors: Taoyong JIN (tyjin@sgg.whu.edu.cn), Hao DING (dhaosgg@sgg.whu.edu.cn)

© Science China Press 2025

in sea level change are still few (the two undisputed signals are ~11 yr and ~18.6 yr) and the ~60-yr signal is currently a hot topic. There is significant controversy regarding its existence, exact period, influence, and possible excitation sources.

The first point of contention about the ~60-yr signal lies in that multiple literature indicate different periods ranging from 50 to 90 years in multiple sea level records, which raises doubts about whether they represent a common oscillation (Scafetta, 2014; Courtillot et al., 2022). An evident 60–65-yr cycle was identified through visual inspection in the reconstructed GMSL (Jevrejeva et al., 2008). From another reconstructed GMSL and regional average sea level, signals of approximately 50–75-yr were found by visual inspection too (Wenzel and Schröter, 2010). Apart from the mean sea level, similar oscillations have been found in various single tide gauge records. Two inflection points roughly in the 1920s–1930s and 1960s were used to describe the interdecadal variation in 14 tide gauge records located in Europe and North America (Woodworth et al., 2009). Remarkable decadal sea level changes up to 15 cm exist on the eastern border of the North Atlantic Ocean and the Mediterranean Sea, which are characterized by 3 marked dips in the 1950s, 1970s and early 1990s (Calafat et al., 2012). An ~60-yr signal was detected visually in the sea level on the northeastern coast of the United States (Sallenger Jr et al., 2012). Kenigson and Han (2014) reported evident oscillations of about 60 yr in the Fourier spectrum of 12 tide gauge records in the "hot spot" area (the highly populated North American Atlantic coast north of Cape Hatteras). Scafetta (2014) found oscillations of approximately 60–70 yr at six globally representative long-term tide gauges. These studies provide different cycles close to 60 years, but lack an evaluation of the uncertainty of these cycles. A major recent development is that Ding et al. (2021a) found a 64±3 yr oscillation at 94 tide gauges worldwide with an array processing technique called optimal sequence estimation (OSE; Ding et al. (2021b)), and further proposed its mathematical model and possible excitation source from the Earth's interior. However, some researchers hold a skeptical attitude toward the ~60-yr signal. Chambers et al. (2012) consider this cycle might be an artificial change caused by seawater redistribution and sparse sampling, but this redistribution process does not affect GMSL. Even if the 60 yr signal exists, its impact on the GMSL is minimal. The deviation caused by neglecting it is less than the uncertainty when estimating the sea level rise rate, so it does not need to be considered. Wahl and Chambers (2016) conducted regression analysis on multidecadal sea level changes at 20 tide gauges in coastal areas of the United States; their findings revealed notable discrepancies and irregularities in the amplitudes and phases of multidecadal variations across different sites. Han et al. (2017) also compared the principal components of sea level changes (mainly interannual and interdecadal changes) and climate modes in four oceans, and obtained a similar conclusion that there are large differences. These results make it doubtful whether the ~60-yr signal has a global distribution or comes from a single excitation source.

Another unresolved issue in the ~60-yr signal related research is its potential excitation sources. Many other time series have similar periodic signals, such as global mean surface air temperature (Schlesinger and Ramankutty, 1994; Wu et al., 2007), Earth's rotation (Mazzarella, 2007), North Pacific sea surface temperature (SST) (Minobe, 1997), reconstruction of tree rings (Delworth and Mann, 2000; Biondi et al., 2001; Gray et al., 2004), Greenland ice cores (Chylek et al., 2012), pole shifts (Ding and Chao, 2018), solar activity records (Veretenenko and Ogurtsov, 2018), North Atlantic SST (Delworth and Mann, 2000), and meteorite fall frequencies (Scafetta et al., 2020). Studies have also shown that this signal seems to be related to many factors, and different regions have different dominant factors. Miller and Douglas (2007) believed this signal might be related to eddy-scale sea surface pressure changes. Jevrejeva et al. (2008) suggested that the signal may be related to changes in the thermohaline cycle caused by density anomaly convection or a combination of vortex and inversion convection. Sturges and Douglas (2011) proposed that a large portion of decadal changes in European sea level are driven by the wind field and propagation of Rossby and/or Kelvin waves. Calafat et al. (2012) attributed most of the signal to coastal wind and wave propagation in the eastern boundary of the North Atlantic and the Mediterranean Sea. Scafetta (2014) believed that the Pacific Decadal Oscillation (PDO), Atlantic Multidecadal Oscillation (AMO), and North Atlantic Oscillation (NAO) all have significant impacts on mutidecadal changes in tide gauge records. According to the existence of a nearly 60-yr vibration in precipitation of North America, Africa and South America, as well as the good correlation between GMSL and AMO, the signal is thought to be a change in ocean mass associated with the global water cycle (Enfield et al., 2001; McCabe et al., 2004; Knight et al., 2006). Scafetta et al. (2020) suggested that the 60-yr cycle in meteorite fall frequency indicates a possible interplanetary dust forcing of the Earth's climate driven by gravitational coupling due to the orbital eccentricity of Jupiter. Ding et al. (2021a) believed that the signal originated from the rotation of the Earth's inner core because both the length of day (LOD) and the geomagnetic field dipole change have almost identical periodic signals. Based on the existing research, the possible sources of the 64-yr signal can be roughly divided into three aspects (which may be coupled or decoupled): the intrinsic mode of the Earth's interior vibration-related factors, such as core motion, geomagnetic field and Earth flattening; astronom-

ical factors, such as sunspots, radiation driving and meteorite fall frequency; and climatic factors, such as temperature, pressure, and the wind field. So far, the most convincing evidence is related to the interior Earth in that the "equivalent excited sequence" of the 64-yr sea level oscillation almost overlaps with the ~64-yr signal in the Earth's magnetic field dipole changes and the backward LOD (Ding et al., 2021a). For solar activity, Veretenenko and Ogurtsov (2018) did not analyze the original sunspot numbers but conducted a correlation spectrum analysis between sunspot numbers and sea level pressure (SLP); however, the ~63-yr peak in their correlation spectrum is possibly due to a relatively high correlation on that time scale but does not necessarily mean that the ~63-yr signal does exist in the two time series.

Overall few studies have carried out spectral analysis to estimate the signal period (Sturges and Douglas, 2011; Kenigson and Han, 2014; Ding et al., 2021a), while most studies simply determine the period by visual scan in the time domain lacking uncertainty assessment, resulting in the estimated period varying greatly between 50 and 90 years. Due to the limited data length, least squares fitting with these different periods may be similar to each other, and it is difficult to distinguish the best one in the time domain, which may cause misleading results (Chambers et al., 2012). In addition, most studies are conducted on a small number of time series from a single station or sea area. 29 global tide gauges were used by Chambers et al. (2012), more than most existing studies, but still relatively few compared to available ones; the average number in each ocean basin is less than five. Ding et al. (2021a) used more stations but presupposed that the signal follows spherical harmonic distribution (one of the many types of spatial distributions which uses the spherical harmonic functions as basis functions) to form only five time series for further analysis. Different from their research, we make no assumptions about this signal and directly analyze it in the time domain instead of the spherical harmonic domain. Additionally, since they proposed the possibility of the Earth's interior excitation source, we analyze the Earth's external excitation sources which have not been fully explored as supplementary.

In this study, global tide gauge records are analyzed separately to detect the possible 64-yr sea level oscillation; the distribution characteristics of the frequencies, amplitudes, and phases of the 64-yr oscillation are analyzed and compared with the mathematical model given by Ding et al. (2021a); seven GMSL time series from different contribution processes are analyzed and compared with the theoretical global mean curve of the 64-yr oscillation; and several long-term geophysical records related to the solar and climate system are also analyzed to confirm whether they are possible excitation sources of the 64-yr sea level oscillation.

## 2. Data and methods

### 2.1 Tide gauge records

Satellite altimetry and tide gauge records are two main techniques to estimate sea level changes. Given that satellite altimetry observations cover only 30 years, detecting inter-decadal and longer periodic signals is challenging. Therefore, 1542 global monthly tide gauge records are downloaded from PSMSL (Permanent Service for Mean Sea Level) in the RLR (Revised Local Reference) datum (Holgate et al., 2017). Although the PSMSL has pre-processed the raw data from the data providers, there are still some problems, so we performed the following operations on the original data:

(1) For low-quality flagged data, most of these data were deleted unless explicitly corrected. Overall, there are 73 mean tide level observations, 18 abnormal tide gauges, 54 records whose description documents contain keywords indicating observation errors, and 77 records described with keywords such as earthquakes, volcanic eruptions, cyclones, etc., indicating actual events. After eliminating those low-quality data, the number of tide gauge records was reduced from 1542 to 1320.

(2) For the datum shift between two segments of data caused by changes in vertical land movement, the correction was directly applied if the offset is classified in the description document. Otherwise, Hector software (Bos et al., 2013) was used to detect the offset; then, the given time was compared with the estimated time when the shift occurs; if the results are consistent, the original data were corrected according to the estimated shift, otherwise deleted. By visual inspection, no significant datum shift was observed in the remaining data.

(3) For potential remaining outliers exceeding 3 times the standard deviation, the outlier removal operation performed by PSMSL for each month of the year separately (a linear fit is made to the time series and any individual value more than 4.5 standard deviations from the fitted line is flagged as an outlier) was extended to a full-time span. A slight modification was made that seasonal cycles were introduced in the linear fitting. As linear trends and seasonal signals dominate sea level changes, this method was effective in removing outliers.

(4) For possible strong correlations between nearby tide gauges, correlation analysis was carried out for tide gauges within 30 km. Two tide gauges were merged into one site if they passed the correlation test. The method of merging is to calculate the difference between the averages of the two observations, take the longer observation as the benchmark, delete data in the shorter observation that covers the same time, and insert the remaining data into the benchmark observation according to the difference above. The threshold was set as the correlation coefficient greater than 0.9 and the

p-value less than 0.1%. After iterative merging, the number of tide gauge records was reduced to 1248.

(5) For a lot of gaps in the records; we discarded those records with data completeness below 70%, and the number of tide gauge records decreased to 1195. From Figure S1, at the 70% threshold, 6 tide gauges longer than 60 years would be removed, while at the 80% threshold, 23 would be removed. A more strict data selection strategy would not affect the final results (nearly the same so not shown) but would increase the uncertainty significantly and lead to a loss of global representativeness, so we adopted the more conservative threshold 70%.

Overall we implemented a conservative data preprocessing approach to preserve as much data as possible while making minimal changes. After preprocessing, a total of 1195 tide gauges remained, of which 845 tide gauge records are longer than 20 yr and 193 records are longer than 65 yr, far more than the number of sites used in existing studies. The spatial distribution of the 845 tide gauges is shown in Figure 1, where the color represents the corresponding data length of each tide gauge (the data length is defined as the number of effective observations divided by 12, and a nonuniform color scale was used to highlight the 193 long-term tide gauge records longer than 60 yr). The 193 long-term tide gauges are distributed in all regions of the world, so they can be considered globally representative. According to the sampling theorem, if an ~60-yr global signal truly exists, it should be theoretically observable at these long-term tide gauges.

### 2.2 Methods of estimating low-frequency signals

Similar to the usual time series analysis frame, tide gauge records were processed in three steps: linear detrending and interpolating, low-pass Gaussian filtering (the cutoff frequency is 0.1 cycle per year), and spectral analysis. For the low-pass filtered time series, the Fourier spectrum was used to preliminarily identify significant peak frequencies above 90% confidence level (Hasselmann, 1976); then around these peak frequencies, a frequency-domain auto-regressive (AR) method called stabilized AR-z was used to estimate accurate periods (Chao and Gilbert, 1980; Ding and Chao, 2018); next invalid periods larger than the data length were discarded; and finally, all of these detected periods were used to fit the low-pass filtered time series. In that way, the periods, amplitudes and phases of all the periodic signals are obtained. Stabilized AR-z was selected to estimate the frequency instead of traditionally selecting peak frequency in the Fourier spectrum or wavelet analysis because of its higher accuracy and higher resolution as proven in Appendix Text S1 and Figure S2 (https://link.springer.com). The basic idea of AR-z is to solve the AR equation in the frequency domain as follows:

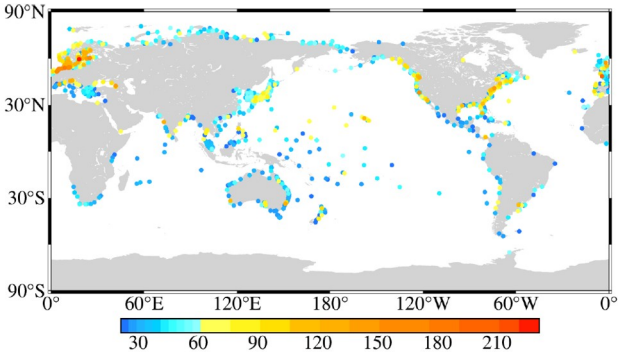


**Figure 1** Spatial distribution of postprocessed tide gauges, where the color scale indicates data length.

$$X_3(\bar{\omega}) = S_1X_1(\bar{\omega}) + S_2X_2(\bar{\omega}), \tag{1}$$

where $X_k$ is the complex Fourier transform of the truncated time series $\mathbf{X}_k=\{x(k), x(k+1), \ldots, x(N+k-3)\}$, $k$=1, 2, 3, $N$ is the whole time series length, and $\bar{\omega}$ are three adjacent frequency points around each peak frequency in the Fourier spectrum. The values of $S_1$ and $S_2$ can be estimated by linear least squares fit. By the Prony relation, the AR coefficients are related to a decaying sinusoidal wave, i.e. the frequency and decay factor follow the equation:

$$\begin{aligned} \omega &= \cos^{-1}\left(S_1/\left(2\sqrt{-S_2}\right)\right), \\ \alpha &= -0.5\ln(-S_2). \end{aligned} \tag{2}$$

The Lorentzien power spectrum in AR-z is defined as follows:

$$P(\bar{\omega}_i) = \frac{1}{\left|e^{j\bar{\omega}_i-\bar{\alpha}_i} - e^{j\omega_i-\alpha_i}\right|^2}, i = 1, 2, \cdots, N, \tag{3}$$

where j is the imaginary unit, and $\bar{\alpha}_i$ is the reference value (usually a very small number close to zero such as 1e–10). This spectrum does not contain information about the actual signal amplitude but can effectively separate different frequencies which will help determine whether there is 64-yr oscillation in the data afterward.

## 3. Results

### 3.1 Existence of the 64-yr signal in multidecadal sea level

For the 845 tide gauges, the above low-frequency signal extraction scheme is performed for each record, and all the significant oscillations' corresponding periods are drawn as scatterplots and statistically counted in Figure 2, along with the mean spectrum. Figure 2 shows the overall distribution characteristics of the multidecadal signals at these tide gauges, where there are 193 tide gauge records longer than 65 years in panel (a) and 652 tide gauge records in panel (b) shorter than 65 years. From panels (a) and (b), there are

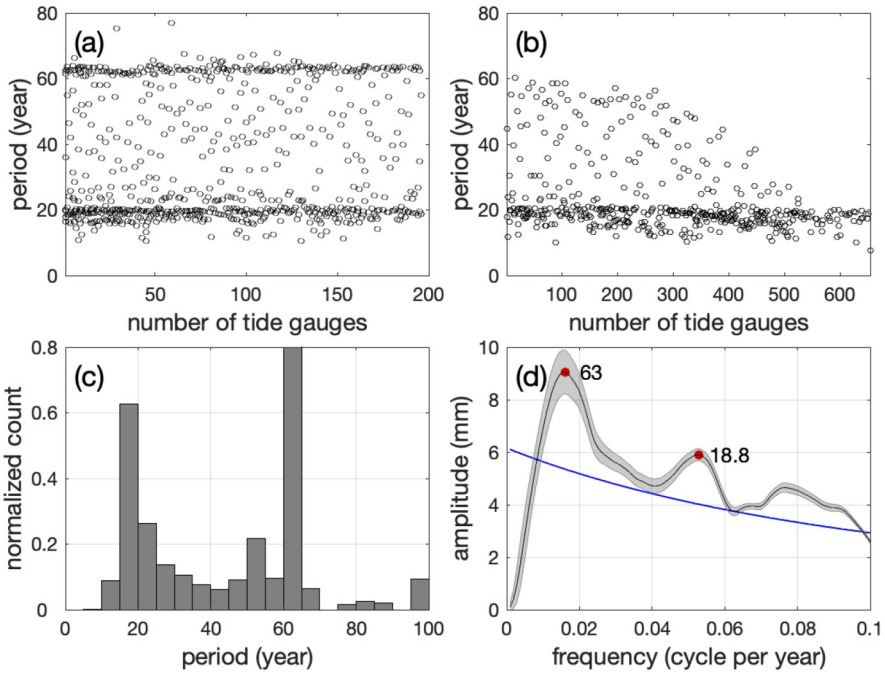


**Figure 2** Scatter distributions (a, b) and histogram (c) of significant periods, and the mean spectrum (d) averaged from global tide gauges. In panels (a) and (b), the tide gauges are arranged in descending order of data length separated by 65 years long. In panel (c), the histogram is normalized by the number of tide gauges long enough to detect the corresponding periods. In panel (d), the black curve is the spectrum, the blue line is the average 90% confidence level line, the red dots represent significant peak signals, the grey area represents the estimation error, and the numbers are the periods corresponding to the peaks.

relatively more period points concentrated around the two lines at ~60 yr and ~20 yr, indicating that the two signals play a significant role in multidecadal sea level changes at these tide gauges, which can also be seen from the two bulges of 15–20 yr and 60–65 yr in Figure 2c. It should be noted that without filtering, many period points will appear in the 0–10 yr frequency band, thus masking the distribution characteristics of period points in the 10–60 yr band, hence, low-pass filtering is necessary.

Similar conclusions can also be reached in the frequency domain. Figure 2d shows the mean spectrum averaged from all tide gauge spectra (three times zero padding was used to smooth the spectra), where the confidence level line was calculated based on red noise assumption (Hasselmann, 1976). The two peaks at 63 yr and 18.8 yr are consistent with the two bulges (60–65 yr, 15–20 yr) in Figure 2c, indicating that the two oscillations exist at many tide gauges and have relatively large amplitudes. The 18.8-yr peak corresponds to the Lunar nodal tide, which is well known in theory; so we will not pay more attention to it. The approximate 60–65-yr oscillation is verified in an average sense above both from the statistically counted histogram and the mean spectrum, the next analysis will be based on this interval. Considering the estimation error caused by noise and the possible bias during detrending and filtering, the periods in the larger interval 58–69 are adopted, as it basically agrees with most estimates and excludes the two subharmonics of Lunar nodal cycle 55.8 and 74.5 (Iz et al., 2018). The approximate 60~65-yr oscillation is significant at 177 tide gauges through the above screening method; the spatial and temporal information of those tide gauges is listed in Table S1 along with their estimated periods. The average period is 63±4 yr (in 90% confidence level), close to the estimate of Ding et al. (2021a) and other studies. Considering that there are only 193 tide gauge records longer than 65 years, it may be concluded that nearly all long-term tide gauges have this approximate 60–65-yr oscillation. A sensitivity analysis on the key parameters including the cutoff frequency of the filter, the interpolation method and the order of the AR model was performed to test the stability of the results under different parameter settings. Nearly the same results as Figure 2 could be obtained, so the figures were not plotted and we only took a tide gauge record (ID: 0005; data completeness: 76%) as an example. The different estimated frequencies under different parameter settings are plotted in Figure S3. It could be seen that although the estimated frequencies vary greatly under different filtering cutoff frequencies and interpolation methods (the order of AR model seems to have little effect), they remain the same within one decimal place. Therefore, we tend to believe our results are stable and insensitive to the parameter setting.

### 3.2 Spatial distributions of the amplitude and phase

For those 177 tide gauges with significant ~64-yr oscillation, their estimated amplitudes and phases (relative to 1980 in-

stead of 0 to avoid large extending bias) are listed in Table S1, and their spatial distributions are shown in Figure 3a and Figure 3d. Although tide gauges with this oscillation are much sparser, their geographic distribution still has global representativeness. It can be seen in Figure 3a and Figure 3d that amplitude/phase seems to depend on latitude/longitude, so the amplitude and phase versus latitude and longitude are drawn in Figure 3b, 3c, 3e and 3f, respectively, to confirm dependence. The amplitude seems symmetrical from north to south, which reaches its largest in the 45° region, and decreases to both sides, while the phase has a longitude-dependent relationship and increases linearly from west to east. This ~64-yr oscillation has a maximum impact of ~20 mm around Western Europe, Eastern Asia, North America and Southern Australia, most of which are densely populated and economically developed areas; however, the sea level contribution from this 64-yr oscillation will keep rising only around North America and Western Europe and decreasing elsewhere according to the phase distribution. Our results are compared with the mathematical model of a spherical harmonic $Y_{2,1}$ spatial pattern proposed by Ding et al. (2021a) shown in eq. (4):

$$u(t,\theta,\lambda) = -\frac{A}{4}\sqrt{\frac{15}{2\pi}}\sin 2\theta \cdot \cos\left(\frac{2\pi t}{T} + \varphi + \lambda\right), \quad (4)$$

where $u$ is sea level at time $t$ (unit in year), colatitude $\theta$ and longitude $\lambda$, $A$ is 47.7 mm, $T$ is 64 yr, and $\varphi$ is −0.406 rad.

As can be seen from Figure 3, although there are some gaps and discontinuities due to limited data coverage, especially in the Southern Ocean, the estimated amplitudes and phases are basically in agreement with the model. The estimated amplitudes and phases (converted to values relative to 1980) from Chambers et al. (2012) are also consistent with the model and our estimated results as shown in Table S2, which suggest the viability of the model and the existence of 64-yr oscillation further. However, large visible differences still exist, probably because different tide gauges are selected, different data preprocessing methods are adopted and other signals were included due to the use of the larger adopting interval. As the oscillation's period is far away from 55.8 yr and 74.5 yr, and does not seem to follow the $Y_{2,0}$ spherical harmonic distribution of Lunar nodal tide, we tend to believe the oscillation is a different real signal rather than a combination of those two subharmonics of Lunar nodal cycle (Iz et al., 2018).

### 3.3 Multidecadal characteristics of different sea level components

According to the mathematical expression in eq. (4), the spherical harmonic model was applied to the global ocean area, and the global mean value of this sea level oscillation can be computed, which resulted in an oscillation curve with the same 64 yr period. The amplitude is about 1 mm, which is small but detectable and not negligible; the phase is about 0.7 rad, indicating that the peak occurred around 1913 and 1977, while the trough occurred around 1945 and 2009, which means that the contribution of this 64-yr oscillation to GMSL will continue to increase and reach its maximum value until 2041. This predicted 64-yr oscillation could lead to an acceleration of ~0.01 mm yr$^{-2}$, which accounts for

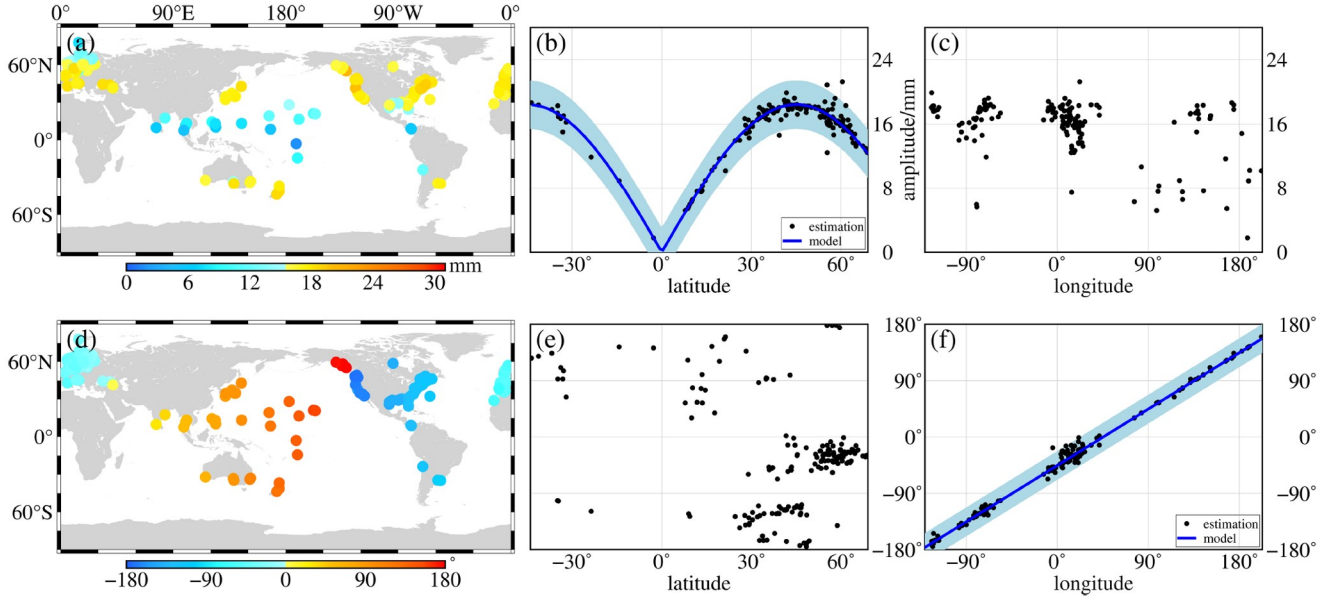


**Figure 3** Spatial distributions of the estimated amplitudes (a) and phases (d), amplitude versus latitude (b), amplitude versus longitude (c), phase versus latitude (e) and phase versus longitude (f) of the ~64-yr oscillation from the estimation (black) and model values (blue), where blue shading represents uncertainty of the model; some values of the longitude and phase add or subtract 360° to make them close to the straight line.

~10% of the total acceleration of ~0.1 mm yr$^{-2}$ in the GMSL from satellite altimetry (Cazenave and Moreira, 2022). Here we attempt to capture the multidecadal characteristics in the other seven GMSL time series contributed from different physical processes, to see if they match the predicted 64-yr oscillation. The seven time series from Frederikse et al. (2020) include GMSL contributed by: ocean thermosteric expansion (caused by variations in ocean temperature), glacier mass loss, Greenland ice sheet mass loss, overall changes in terrestrial water storage (TWS), water impoundment in artificial reservoirs, groundwater depletion and changes in natural TWS. For most of the time series, linear detrending or parabolic detrending is enough which will not affect the final results in the common sense. For the glacier data, a continuous piecewise fit with a linear trend before 1963 and a parabolic trend after 1963 was performed as shown in Figure S4. It could be seen that the fitted trend could well capture the overall signal and there is no problem of trend changes in the detrended time series, which means that our detrending is accurate and has a negligible effect on the final result. These detrended time series and their corresponding wavelet transforms are shown in Figure 4, and the predicted 64-yr oscillations are plotted as well. It can be seen that none of these time series' multidecadal characteristics match the predicted 64-yr oscillation both in amplitude and phase, and their main periods are distinct from 64 yr in the wavelet transform, which is clearer in their AR-z spectrum in Figure S5. In addition to time series analysis for the seven GMSL components, OSE is performed for gridded steric sea level change, and the spherical-harmonic stack series and the corresponding AR-z spectrum are shown in Figure S6; but no 64-yr signal was found either especially in the spherical harmonic item $Y_{2,1}$. These seven GMSL time series are related to the ocean mass change and ocean density change forced by climate change, but do not include the forced vibrations from wave propagation. Therefore we tend to believe the 64-yr oscillation is not contributed by ocean thermal expansion (at least the $Y_{2,1}$ spatial pattern is not related to the thermosteric sea level change) or other climatic/artificial factors (sea level change caused by large-scale mass change does not follow the $Y_{2,1}$ spatial pattern), but a kind of wave transmitted from elsewhere such as interior Earth through angular momentum exchange (Yang and Song, 2023).

### 3.4 Possible excitation source of the 64-yr oscillation

To confirm or exclude the possible excitation source of the 64-yr signal, seven representative observations are analyzed here, including sunspot numbers, 10.7 cm solar flux data, reconstruction of total solar irradiance (TSI, there are three reconstructions but they are similar as shown in Figure S7, so only one TSI@1 is analyzed here) (Scafetta, 2023), zonal index of pressure (Mazzarella and Scafetta, 2018), global mean precipitation (Dai et al., 1997), global mean SLP (Allan and Ansell, 2006) and global mean surface temperature (Morice et al., 2021), in which the first three time series are related to solar activity and the last four time series are related to the climate system. Those initial/detrended time series and their wavelet transforms are shown in Figure 5, including the predicted 64-yr oscillation, whose amplitude in each panel was adjusted to be the standard deviation of the corresponding time series. It can be seen that there is no evident 64-yr signal in most of the time series and the wavelet transform, which is clearer in their AR-z spectra in Figure S7 that those frequency peaks are far away from 64 years. The estimated periods closest to 64 yr of the seven time series are 54, 43, 53, 80, 41, 39 and 54 years, respectively. The differences between these values and 64 range from −25 to 16, with a standard deviation of 14 (far beyond our estimate of 64±3), making it difficult to consider them as the same signal. As the amplitude-adjusted predicted 64-yr oscillation seems to fit the zonal index well with a phase lag and oscillates in the antiphase with the global mean temperature, we tried to exclude the existence of the 64-yr signal in these two time series. The detailed argumentation, whose basic idea is from Ding (2023), is displayed in Appendix Text S2, Figure S9 and Figure S10. Nine representative climate indices covering different areas around the world were also analyzed by AR-z in Figure S11 including the AMO (Cai et al., 2024), PDO, Antarctic Oscillation (AAO), Arctic Oscillation (AO), Dipole Mode Index in the Indian Ocean (DMI), Greenland Blocking Index (GBI), multivariate ENSO index (MEI), Interdecadal Pacific Oscillation (IPO) and Southern Annular Mode (SAM). No 64-yr signal was found in any of them either. This result is expected, as climate indices fundamentally influence sea level through temperature and pressure. Since neither temperature nor pressure data exhibit this signal, it makes sense that the climate indices would not either. As no single climate index exhibits the 64-yr signal, their linear combinations cannot produce such a signal; if their combined impacts are nonlinear, it is also nearly impossible to generate a consistent global signal with standard oscillation (nonlinearity is often related to irregularity). According to these results, we may conclude that the 64-yr signal is not widespread in solar activity or the climate system, therefore the signal is not likely to be excited by the two Earth external sources. The ~60-yr signal found in other climate indices of the climate system and meteorite fall frequency is probably a different signal due to gravitational coupling from the orbital eccentricity of Jupiter or something else (Scafetta et al., 2020).

## 4. Conclusions

Research on low-frequency sea level changes is of both

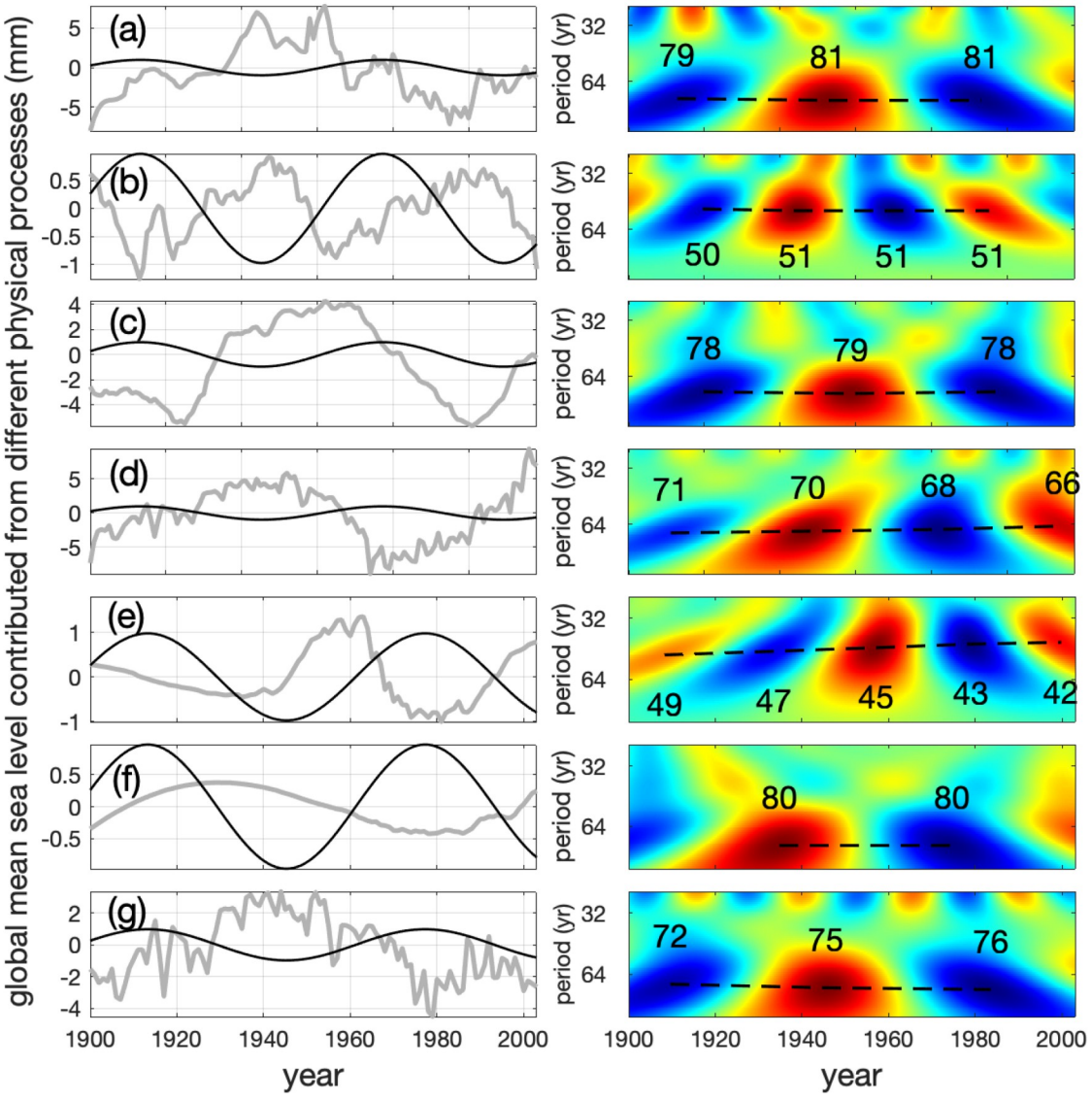


**Figure 4** Seven different detrended GMSL time series (left grey line) and the corresponding wavelet transform (right) contributed from ocean thermosteric expansion (a), glacier mass loss (b), Greenland ice sheet mass loss (c), overall changes in TWS (d), water impoundment in artificial reservoirs (e), groundwater depletion (f) and changes in natural TWS (g), where the black line on the left is the predicted 64-yr oscillation and the numbers in the wavelet transform are the periods near 64 years.

theoretical and practical significance. However, there is limited global analysis of the specific period, amplitude and phase of multidecadal changes, especially the ~60-yr signal. In this work, as an extension of the spherical harmonic domain analysis in Ding et al. (2021a), the global 64-yr sea level oscillation is verified in the time domain independently using many more tide gauge records, and the Earth's external excitation sources are excluded supporting their hypothesis regarding the Earth's internal sources.

Global tide gauge records have been finely processed, and the number of tide gauges, spatial distribution and time span have been greatly improved. According to the global tide gauges' mean frequency spectrum, scatter diagram and histogram of the significant frequency points, the 64-yr oscillation is confirmed. The period determined in this paper is 63±4 yr, the uncertainty is large but basically agrees with other estimates. The global distributions of amplitude and phase shows that the amplitude is dependent on latitude while the phase is dependent on longitude. At the regional scale, the 64-yr sea level oscillation can reach ~20 mm, which has a significant effect on the local sea level and should be considered when estimating regional sea level rise parameters particularly for highly-populated midlatitude coastal areas, such as the 'hotspot' area and eastern Australia for the next 30 years. On a global scale, the amplitude of the predicted 64yr oscillation is ~1 mm, much smaller but still not negligible and could account for ~10% of the total acceleration in the GMSL from satellite altimetry; the phase is

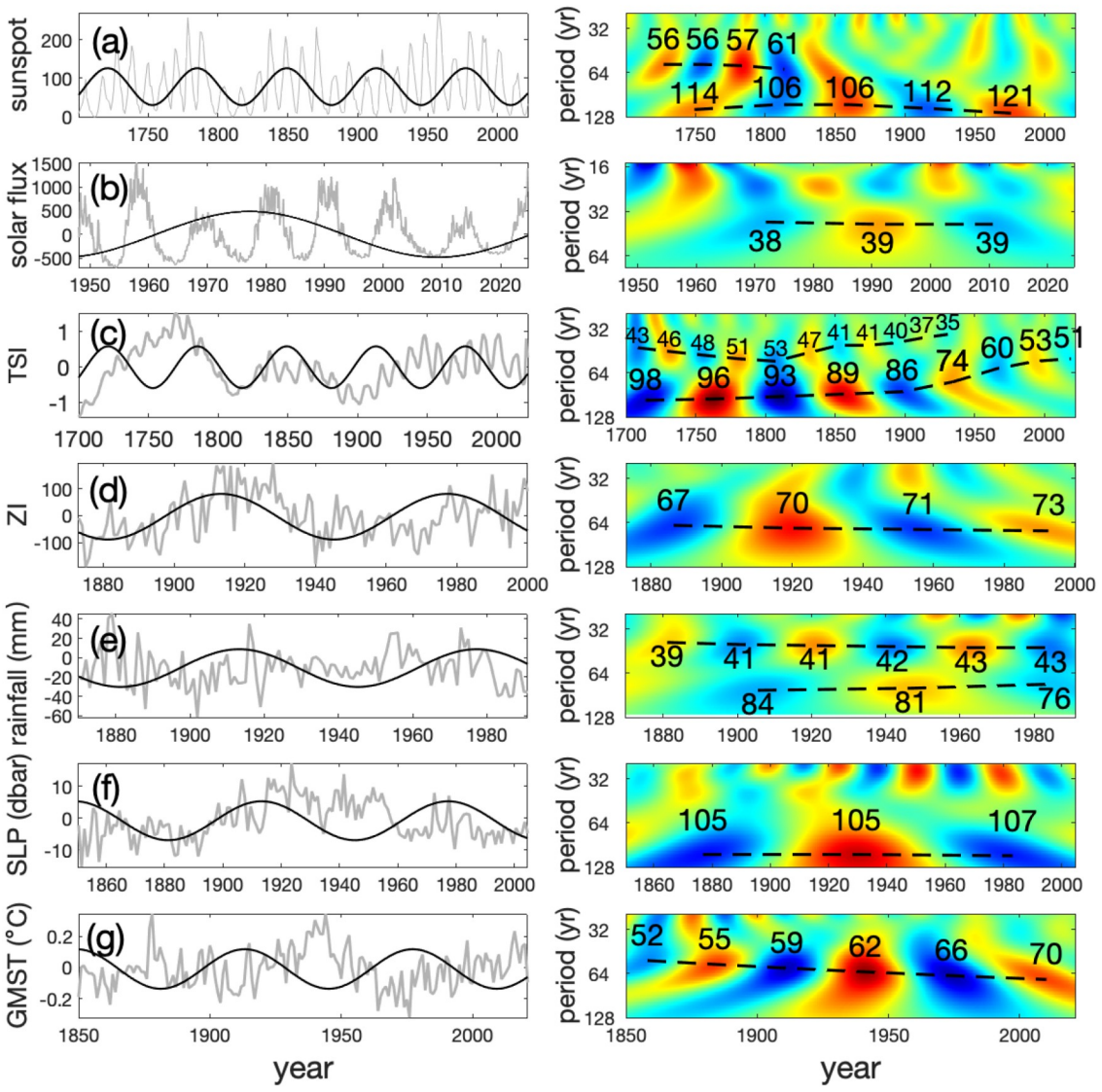


**Figure 5** Initial/detrended time series (left) and the corresponding wavelet transform (right) of sunspot numbers (a), 10.7 cm solar flux data (b), TSI@1 (c), zonal index of pressure(d), global mean precipitation (e), global mean SLP (f) and global mean surface temperature (g), where the black lines on the left represent the amplitude-adjusted predicted 64-yr oscillation and the numbers in the wavelet transform are the periods near 64 years.

~0.7 rad, which means the contribution of the 64-yr oscillation to the GMSL will continue growing until 2041. Seven GMSL time series contributed from mainly thermosteric expansion and mass change are analyzed using wavelet transform and AR-z spectrum, but the 64-yr oscillation was not found in any of them; moreover, none of these time series' multidecadal characteristics match the predicted 64-yr oscillation both in amplitude and phase. Therefore we believe the 64-yr sea level oscillation is not related to thermosteric sea level or ocean mass changes but a kind of forced vibrations transmitted from elsewhere. To further confirm or exclude the possible excitation sources, seven representative solar-related and climatic geophysical records closely related to sea level were also analyzed. Although there seem to be 64-yr cycles in the wavelet transform of some datasets, they are not actually 64 years in the more precise AR-z spectrum. As for the zonal index and global mean surface temperature whose multidecadal characteristics seem to match the predicted 64-yr oscillation, we excluded their 64-yr oscillation by comparing different fitting effects in the frequency domain. Through the above analysis, we suggest the 64-yr oscillation is not excited by the external sources of solar activity and the climate system. Although the exact source is still unknown, we tend to believe the oscillation originates from internal Earth and the ~60-yr cycle found elsewhere is probably a different signal. However, a more accurate and quantitative explanation needs longer data and much further work.

The verified 64-yr oscillation approximately obeys spherical harmonic distribution. However, large visible differ-

ences still exist, probably because of different data selections and/or different data processing methods, so a more detailed analysis needs to be carried out on a regional scale to explain the difference as well as the influence of the signal on relative sea level rise. Apart from the two frequencies detected in this paper, there are probably more other low-frequency signals in sea level change; thus, special processing is required for potential signals in the future. The impact of vertical land motion is simplified as a linear trend here which may cause bias, this item needs to be more carefully considered too. In addition, more other types of relevant observations are required to analyze and interpret the detected signals in order to give mechanism explanations and carry out reasonable physical modeling. In particular, there is a possibility that periodic internal Earth motion excites shear deformation in the seafloor, leading to vertical movements of seawater, i.e., sea level changes. This would require more detailed observations of the ocean's gravitational field, seafloor topography, and ocean bottom pressure, as well as a more refined Earth model. Also, there may be yet unknown mechanisms in the climate system which could produce this 64-yr oscillation, such as changes in atmospheric angular momentum leading to similar periodic fluctuations in sea level. This requires longer observational data to reach a definitive conclusion, or a detailed analysis of the CMIP6 data could be considered as an alternative.

**Acknowledgements** *All data used in this paper are publicly available. The tide gauge records were downloaded from PSMSL; the seven GMSL time series were downloaded from Frederikse et al. (2020); the sunspot number was downloaded from https://www.sidc.be/silso/datafiles; the 10.7 cm solar flux data was downloaded from https://psl.noaa.gov/data/timeseries/monthly/SOLAR/; the three reconstructions of TSI were downloaded from Scafetta (2023); the zonal index was downloaded from Mazzarella and Scafetta (2018); the global mean precipitation data was downloaded from https://data.giss.nasa.gov/precip_dai/; the global mean SLP and global mean temperature were downloaded from https://hadleyserver.metoffice.gov.uk/; the AMO and IPO were downloaded from Cai et al. (2024); the AO (Zhou et al., 2001), AAO (Gong and Wang, 1999), DMI (Saji and Yamagata, 2003), GBI (Hanna et al., 2016), MEI (Wolter and Timlin, 2011), PDO (Newman et al., 2016), and SAM (Thompson and Wallace, 2000) were downloaded from https://psl.noaa.gov/data/climateindices/list/ and https://psl.noaa.gov/data/20thC_Rean/timeseries/ (Compo et al., 2011). This study was supported by the National Natural Science Foundation of China (Grant Nos. 42388102, 42192531 & 42374035), the Fundamental Research Funds for the Central Universities (Grant No. 2042023kfyq01), and the Special Fund of Hubei Luojia Laboratory (Grant Nos. 220100001 & 220100002).*

**Conflict of interest** The authors declare that they have no conflict of interest.

## References

Allan R, Ansell T. 2006. A new globally complete monthly historical gridded mean sea level pressure dataset (HadSLP2): 1850–2004. J Clim, 19: 5816–5842

Biondi F, Gershunov A, Cayan D R. 2001. North Pacific decadal climate variability since 1661. J Clim, 14: 5–10

Boretti A. 2020. Relative sea-level rise and land subsidence in Oceania from tide gauge and satellite GPS. Nonlin Eng, 9: 175–193

Bos M S, Fernandes R M S, Williams S D P, Bastos L. 2013. Fast error analysis of continuous GNSS observations with missing data. J Geod, 87: 351–360

Cai Q, Chen W, Chen S, Xie S P, Piao J, Ma T, Lan X. 2024. Recent pronounced warming on the Mongolian Plateau boosted by internal climate variability. Nat Geosci, 17: 181–188

Calafat F M, Chambers D P, Tsimplis M N. 2012. Mechanisms of decadal sea level variability in the eastern north Atlantic and the Mediterranean Sea. J Geophys Res, 117: 2012JC008285

Cazenave A, Moreira L. 2022. Contemporary sea-level changes from global to local scales: A review. Proc R Soc A, 478: 20220049

Chambers D P, Merrifield M A, Nerem R S. 2012. Is there a 60-year oscillation in global mean sea level? Geophys Res Lett, 39: 2012GL052885

Chao B F, Gilbert F. 1980. Autoregressive estimation of complex eigenfrequencies in low frequency seismic spectra. Geophys J Int, 63: 641–657

Chylek P, Folland C, Frankcombe L, Dijkstra H, Lesins G, Dubey M. 2012. Greenland ice core evidence for spatial and temporal variability of the Atlantic Multidecadal Oscillation. Geophys Res Lett, 39: 1–6

Compo G P, Whitaker J S, Sardeshmukh P D, Matsui N, Allan R J, Yin X, Gleason B E, Vose R S, Rutledge G, Bessemoulin P, Brönnimann S, Brunet M, Crouthamel R I, Grant A N, Groisman P Y, Jones P D, Kruk M C, Kruger A C, Marshall G J, Maugeri M, Mok H Y, Nordli Ø, Ross T F, Trigo R M, Wang X L, Woodruff S D, Worley S J. 2011. The twentieth century reanalysis project. Q J R Meteorol Soc, 137: 1–28

Courtillot V, Le Mouël J L, Lopes F, Gibert D. 2022. On sea-level change in coastal areas. J Mar Sci Eng, 10: 1871

Dai A, Fung I Y, Del Genio A D. 1997. Surface observed global land precipitation variations during 1900–88. J Clim, 10: 2943–2962

Delworth T L, Mann M E. 2000. Observed and simulated multidecadal variability in the northern hemisphere. Clim Dyn, 16: 661–676

Ding Hao. 2023. How to extract the ~64 yr signal from the geomagnetic coefficient g1,0. Research Gate, : 1–6

Ding H, Chao B F. 2018. Application of stabilized AR-z spectrum in harmonic analysis for geophysics. J Geophys Res-Solid Earth, 123: 8249–8259

Ding H, Jin T Y, Li J C, Jiang W P. 2021a. The contribution of a newly unraveled 64 years common oscillation on the estimate of present-day global mean sea level rise. J Geophys Res-Solid Earth, 126: e2021JB022147

Ding H, Xu X, Pan Y, Li M. 2021b. Array processing techniques for analyzing global geophysical observation networks: Comprehensive analysis and typical applications. Earth-Sci Rev, 221: 103807

Douglas B C. 1992. Global sea level acceleration. J Geophys Res, 97: 12699–12706

Enfield D B, Mestas-Nuñez A M, Trimble P J. 2001. The Atlantic Multidecadal Oscillation and its relation to rainfall and river flows in the continental U.S. Geophys Res Lett, 28: 2077–2080

Frederikse T, Landerer F, Caron L, Adhikari S, Parkes D, Humphrey V W, Dangendorf S, Hogarth P, Zanna L, Cheng L, Wu Y H. 2020. The causes of sea-level rise since 1900. Nature, 584: 393–397

Gong D, Wang S. 1999. Definition of Antarctic oscillation index. Geophys Res Lett, 26: 459–462

Gray S T, Graumlich L J, Betancourt J L, Pederson G T. 2004. A tree-ring based reconstruction of the Atlantic Multidecadal Oscillation since 1567 A.D. Geophys Res Lett, 31: 2004GL019932

Han W, Meehl G A, Stammer D, Hu A, Hamlington B, Kenigson J, Palanisamy H, Thompson P. 2017. Spatial patterns of sea level variability associated with natural internal climate modes. Surv Geophys, 38: 217–250

Hanna E, Cropper T E, Hall R J, Cappelen J. 2016. Greenland blocking index 1851–2015: A regional climate change signal. Intl J Clim, 36: 4847–4861

Hasselmann K. 1976. Stochastic climate models part I. Theory. Tellus A-Dynamic Meteorol Oceanogr, 28: 473
Holgate S J, Matthews A, Woodworth P L, Rickards L J, Tamisiea M E, Bradshaw E, Foden P R, Gordon K M, Jevrejeva S, Pugh J. 2017. New data systems and products at the Permanent Service for Mean Sea Level. J Coast Res, 38: 217–250
Iz H B, Shum C K, Kuo C Y. 2018. Sea level accelerations at globally distributed tide gauge stations during the satellite altimetry era. J Geodetic Sci, 8: 130–135
Jevrejeva S, Moore J C, Grinsted A, Woodworth P L. 2008. Recent global sea level acceleration started over 200 years ago? Geophys Res Lett, 35: 2008GL033611
Kenigson J S, Han W. 2014. Detecting and understanding the accelerated sea level rise along the east coast of the United States during recent decades. J Geophys Res-Oceans, 119: 8749–8766
Knight J R, Folland C K, Scaife A A. 2006. Climate impacts of the Atlantic Multidecadal Oscillation. Geophys Res Lett, 33: L17706
Mazzarella A. 2007. The 60-year solar modulation of global air temperature: The Earth's rotation and atmospheric circulation connection. Theor Appl Climatol, 88: 193–199
Mazzarella A, Scafetta N. 2018. The Little Ice Age was 1.0–1.5°C cooler than current warm period according to LOD and NAO. Clim Dyn, 51: 3957–3968
McCabe G J, Palecki M A, Betancourt J L. 2004. Pacific and Atlantic ocean influences on multidecadal drought frequency in the United States. Proc Natl Acad Sci USA, 101: 4136–4141
Miller L, Douglas B C. 2007. Gyre-scale atmospheric pressure variations and their relation to 19th and 20th century sea level rise. Geophys Res Lett, 34: 2007GL030862
Minobe S. 1997. A 50–70 year climatic oscillation over the north Pacific and north America. Geophys Res Lett, 24: 683–686
Morice C P, Kennedy J J, Rayner N A, Winn J P, Hogan E, Killick R E, Dunn R J H, Osborn T J, Jones P D, Simpson I R. 2021. An updated assessment of near-surface temperature change from 1850: The HadCRUT5 data set. J Geophys Res-Atmos, 126: e2019JD032361
Newman M, Alexander M A, Ault T R, Cobb K M, Deser C, Di Lorenzo E, Mantua N J, Miller A J, Minobe S, Nakamura H, Schneider N, Vimont D J, Phillips A S, Scott J D, Smith C A. 2016. The Pacific decadal oscillation, revisited. J Clim, 29: 4399–4427
Saji N H, Yamagata T. 2003. Possible impacts of Indian Ocean Dipole mode events on global climate. Clim Res, 25: 151–169
Sallenger Jr A H, Doran K S, Howd P A. 2012. Hotspot of accelerated sea-level rise on the Atlantic coast of north America. Nat Clim Change, 2: 884–888
Scafetta N. 2014. Multi-scale dynamical analysis (MSDA) of sea level records versus PDO, AMO, and NAO indexes. Clim Dyn, 43: 175–192
Scafetta N. 2023. Empirical assessment of the role of the Sun in climate change using balanced multi-proxy solar records. Geosci Front, 14: 101650
Scafetta N, Milani F, Bianchini A. 2020. A 60-year cycle in the meteorite fall frequency suggests a possible interplanetary dust forcing of the Earth's climate driven by planetary oscillations. Geophys Res Lett, 47: e2020GL089954
Schlesinger M E, Ramankutty N. 1994. An oscillation in the global climate system of period 65–70 years. Nature, 367: 723–726
Sturges W, Douglas B C. 2011. Wind effects on estimates of sea level rise. J Geophys Res, 116: C06008
Thompson D W J, Wallace J M. 2000. Annular modes in the extratropical circulation. Part I: Month-to-month variability. J Clim, 13: 1000–1016
Veretenenko S V, Ogurtsov M G. 2018. 60-year cycle in the Earth's climate and dynamics of correlation links between solar activity and circulation of the lower atmosphere. Geomagn Aeron, 58: 973–981
Wahl T, Chambers D P. 2016. Climate controls multidecadal variability in U. S. extreme sea level records. J Geophys Res-Oceans, 121: 1274–1290
Wenzel M, Schröter J. 2010. Reconstruction of regional mean sea level anomalies from tide gauges using neural networks. J Geophys Res, 115: C08013
Wolter K, Timlin M S. 2011. El Niño/Southern Oscillation behaviour since 1871 as diagnosed in an extended multivariate ENSO index (MEI.Ext). Intl J Clim, 31: 1074–1087
Woodworth P L, White N J, Jevrejeva S, Holgate S J, Church J A, Gehrels W R. 2009. Evidence for the accelerations of sea level on multi-decade and century timescales. Intl J Clim, 29: 777–789
Wu Z, Huang N E, Long S R, Peng C K. 2007. On the trend, detrending, and variability of nonlinear and nonstationary time series. Proc Natl Acad Sci USA, 104: 14889–14894
Yang Y, Song X. 2023. Multidecadal variation of the earth's inner-core rotation. Nat Geosci, 16: 182–187
Zhou S, Miller A J, Wang J, Angell J K. 2001. Trends of NAO and AO and their associations with stratospheric processes. Geophys Res Lett, 28: 4107–4110

(Editorial handling: Jiancheng SHI)